RSC Advances

PAPER

View Article Online
View Journal | View Issue

Cite this: *RSC Adv.*, 2020, **10**, 5183

Tailoring the $AlCl_3/iPr_2O/Et_2O$ initiation system for highly reactive polyisobutylene synthesis in pure *n*-hexane

Dan Xie, Shan Zhu and Yangcheng Lu*

This paper reports the flow synthesis of highly reactive polyisobutylenes (HRPIBs) in pure *n*-hexane using properly prepared $AlCl_3 \cdot Et_2O$ crystals in conjunction with $AlCl_3 \cdot iPr_2O$ solution as coinitiators. By preparing $AlCl_3 \cdot iPr_2O$ solution and $AlCl_3 \cdot Et_2O$ crystals separately, the cationic polymerization of isobutylene proceeded smoothly under a wide range of monomer concentrations (0.33–1.30 M) in the presence of H_2O as an initiator, affording a high yield (~89%) and a moderate exo-olefin terminal group content (60–75%) in 10 min. The various functions of iPr_2O and Et_2O in the initiator solution were comprehensively revealed from the polymerization results, attenuated total reflection-Fourier transform infrared and ^{27}Al nuclear magnetic resonance spectra, and density functional theory simulations. $AlCl_3 \cdot iPr_2O$ was confirmed to be the key component that stabilized carbenium ions. The $AlCl_3 \cdot Et_2O$ complex was the key component to promote proton elimination. Free Et_2O should be removed to inhibit its negative effect on isomerization. This new strategy may lead to high commercial interest in HRPIB synthesis in pure green solvent and could potentially be extended to other initiation systems containing solid Lewis acids.

Received 30th December 2019
Accepted 24th January 2020

DOI: 10.1039/c9ra11003h

rsc.li/rsc-advances

Introduction

Polyisobutylenes (PIBs), the most important industrial products of cationic polymerization, are characterized by their thermal stability, flexibility at ambient temperature, and impermeability to gases.[1–5] Therefore, PIBs have been widely used in automobile tires, medical bottle plugs, additives of fuels, and lubricants.[6–9] Highly reactive polyisobutylenes (HRPIBs),[10,11] which are PIBs with high contents of exo-olefin end groups (≥60 mol%) and a specific molecular weight distribution (M_n = 500–5000), are highly reactive intermediates in the preparation of additives for lubricants and fuels. Thus, HRPIBs attract considerable attention from both industry and academia. The commercial synthesis of HRPIBs is dominated by the cationic polymerization of isobutylene (IB) using BF_3 as a coinitiator and traces of alcohol or water as an initiator at temperatures slightly below 0 °C in *n*-hexane.[10,12] However, BF_3 is costly and strongly corrosive, resulting in serious economic and safety concerns.[13]

In a series of publications, novel and economic catalyst systems were reported to produce HRPIBs with high exo-olefin content,[14] such as $FeCl_3$/iPrOH,[8,15] $FeCl_3/iPr_2O$,[7,16–18] and $AlCl_3$/ether. Among the various coinitiators, solid $AlCl_3$ has the advantages of low cost and high activity; however, it is always accompanied by the use of chlorinated solvents like CH_2Cl_2,[9,19–26] at least in the preparation of initiator solution. Considering the environmental and health impacts of chlorinated solvents, it is highly desirable to completely replace them with green solvents such as *n*-hexane. However, the low stability of the carbenium ions in nonpolar solvents generally results in low conversion and poor controllability,[27] making it difficult to effectively obtain HRPIBs in pure *n*-hexane.

The proper stabilization of carbenium ions and effective β-proton elimination, which are known as the keys to preparing HRPIBs,[21,23,25,28,29] depend on the careful regulation of active centers and chain reactions. Our previous investigations have shown that introducing nucleophilic reagents into the initiator solution is an effective and direct method to adjust the active centers and chain reactions when using $AlCl_3$ as a coinitiator.[29–31] In detail, strongly basic Et_2O can decrease the acidity of $AlCl_3$ *via* complexation and inhibit its catalysis of H_2O dissociation, which can stabilize carbenium ions and decrease the polymerization rate in CH_2Cl_2/*n*-hexane solvent mixtures. Meanwhile, the free Et_2O significantly promotes proton elimination and isomerization, resulting in a high conversion rate and a low content of exo-olefin. Similarly, iPr_2O can stabilize carbenium ions and promote proton elimination in CH_2Cl_2. However, iPr_2O has little influence on isomerization due to steric hindrance, leading to a high content of exo-olefin.[32] From these results, it can be concluded that Et_2O may have a stronger influence on the rate of β-H abstraction in pure *n*-hexane, while iPr_2O may better stabilize the carbocations.

State Key Laboratory of Chemical Engineering, Department of Chemical Engineering, Tsinghua University, Beijing 100084, China. E-mail: luyc@tsinghua.edu.cn; Fax: +86 10 62773017; Tel: +86 10 62773017

Herein, we present a novel and simple method to prepare effective initiation solutions in *n*-hexane with a special focus on the synergistic effects of nucleophilic reagents (iPr_2O and Et_2O) on $AlCl_3$-catalyzed IB polymerization. HRPIBs with high conversion rates and exo-olefin contents were successfully synthesized by comprehensively regulating carbenium ion stability, reactivity, and proton elimination. Moreover, attenuated total reflection-Fourier transform infrared (ATR-FTIR) spectroscopy, and ^{27}Al nuclear magnetic resonance (NMR) spectroscopy were combined with density functional theory (DFT) simulation to reveal how the controlled polymerization process was achieved in pure *n*-hexane.

Experimental methods

Materials

n-Hexane (C_6H_6, 97.5+%, anhydrous), isopropyl ether (iPr_2O, 99.0+%), and aluminum chloride ($AlCl_3$, 99+%, anhydrous) were purchased from J&K Scientific (China). Diethyl ether (Et_2O, 99.5+%) and ethanol (analytical reagent) were obtained from Sinopharm Chemical Reagent Co. Ltd (China). IB (99.9+%, anhydrous) was obtained from Dalian Special Gases Co., LTD (China) and used directly as received. *n*-Hexane was dried over Solvent Purification Assembly (VAC, USA), and the content of water was determined using a coulometric Karl Fischer moisture meter (Mettler Toledo, Switzerland). iPr_2O and Et_2O were distilled to remove stabilizer and then dried over Molecular Sieves 5A overnight. iPr_2O, Et_2O, $AlCl_3$, and *n*-hexane were preserved in a glovebox (Mikrouna, China). The content of $AlCl_3$ in the initiator solution was measured by ultraviolet-visible spectrophotometry (UV-2450, Shimadzu).

Polymerization of IB

The polymerization of IB was performed in a microflow system composed of three T-shaped micromixers (M1 for the mixing of IB and diluent in *n*-hexane; M2 for the mixing of IB solution and initiator solution; and M3 for the injection of terminator agent in ethanol), two precooling (or preheating) coiled stainless tubes (C1 and C2, inner diameter = 900 μm), and a microtube reactor (R, inner diameter = 900 μm), as shown in Fig. 1. The polymerization of IB proceeded in R1, and the reaction time could be adjusted by the flow rate and the length of R1. Four syringe pumps were used to deliver IB, *n*-hexane, initiator solution, and terminator at flow rates of 2, 6, 8, and 2 mL min^{-1}, respectively. IB was transferred as a liquid from the bottom of the IB cylinder into the syringe and then mixed with *n*-hexane in the tube as a liquid under a pressure of 3 bar.[29,31]

Preparation of initiation solution

The initiation solution was prepared just before polymerization in a glove box under an argon atmosphere. Seven preparation methods with single or double ethers were studied in this work. (a) Method 1: dry *n*-hexane was added to $AlCl_3$ powder, and then slight excess Et_2O was added to form the initial solution. (b) Method 2: dry *n*-hexane was added to $AlCl_3$ powder, and then slight excess iPr_2O was added. Since $AlCl_3$ powder could not be completely dissolved in this case, the upper layer was withdrawn as an initiation solution, denoted as solution A. (c) Method 3: dry *n*-hexane was added to $AlCl_3$ powder, and an appropriate amount of Et_2O was then added. After several minutes, dry iPr_2O was added. The solution was used as an initiation solution. (d) Method 4: dry *n*-hexane was added to $AlCl_3$ powder, and then an appropriate amount of iPr_2O was added. After stirring for 2 h, dry Et_2O was added. The solution was used as an initiation solution. (e) Method 5: dry Et_2O was added into solution A to form the initial solution. (f) Methods 6 and 7. Dry Et_2O (method 6), *n*-hexane/Et_2O mixture [5/2 (v/v), method 7], or separate *n*-hexane and Et_2O (method 7–1) was added to $AlCl_3$ powder and then vacuumed to form a colorless crystal B. Solution A was added to crystal B under stirring to form the initiation solution (Fig. 2).

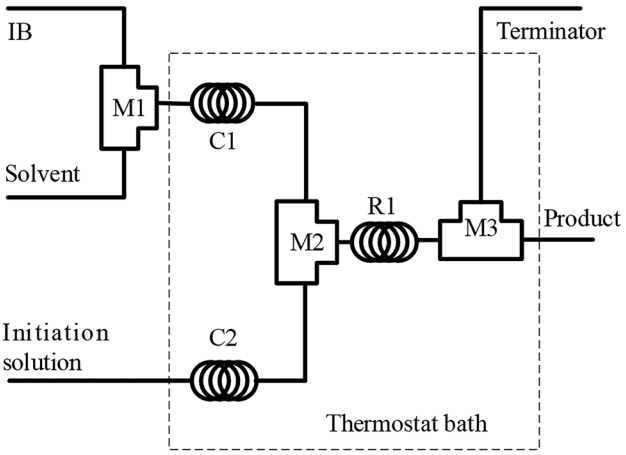

Fig. 1 Schematic diagram of the flow synthesis setup. M1, M2, and M3 are T-shaped micromixers; C1 and C2 are curved tubes for achieving the pre-set temperature; and R1 is a microtube reactor.

Characterization

Size-exclusion chromatography. The molecular weight and dispersity value ($Đ$) of the polymers were measured using a Waters gel permeation chromatography (GPC) system compromised of a Waters 2707 autosampler, a 1515 Isocratic high-performance liquid chromatography pump, a 2414 refractive index detector, and three Styragel GPC columns [Styragel HT3, HT4, HT5; column size = 7.8 × 300 mm; particle size = 10 μm]. The molecular weight could be detected in the range of 500–4 × 10^6. The system was thermostated at 38 °C. Tetrahydrofuran was used as the eluent at a flow rate of 1.0 mL min^{-1}. The instrument was calibrated with polystyrene standards. The results were processed by Breeze 2 software (Waters).

ATR-FTIR spectroscopy. The ATR-FTIR spectra were recorded *in situ* using a Mettler Toledo ReactIR 15 instrument with a DiComp probe coupled to a mercury cadmium telluride detector *via* AgX fiber. Each spectrum was collected every 256 s by accumulating 256 scans with a wavenumber resolution of 4 cm^{-1} over the spectral range of 650–3000 cm^{-1}. The ATR-FTIR

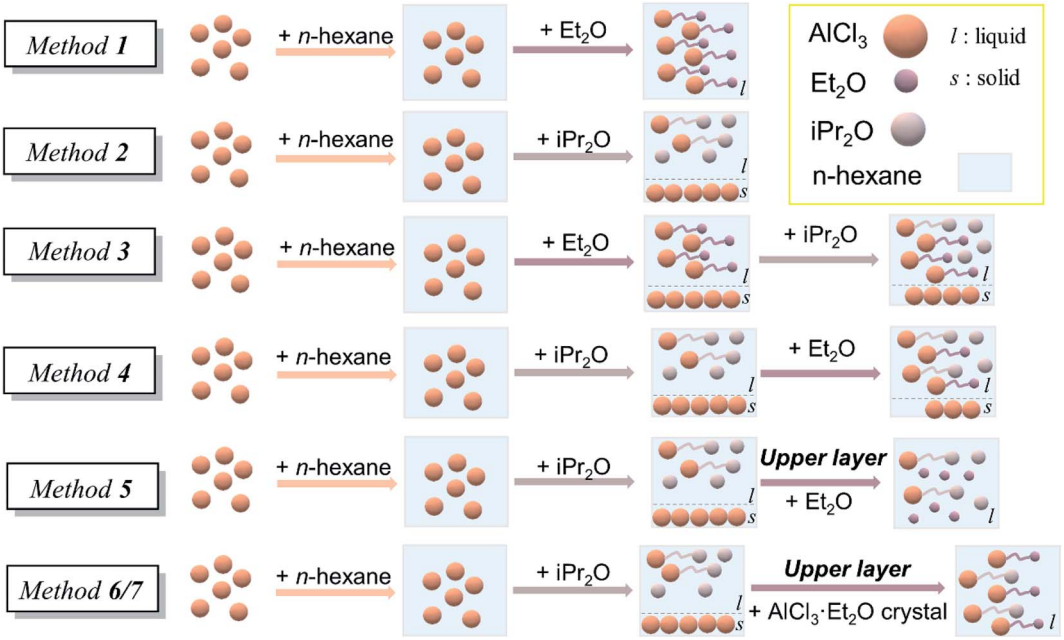

Fig. 2 Schematic of various preparation methods of initiation solution.

spectrum of diluent (*n*-hexane or CH_2Cl_2) was chosen as the background. The measurement temperature was 25 °C.

NMR spectroscopy. The ^{27}Al NMR spectra were measured using a JNM-ECA 600 MHz spectrometer using $[Al(OD)_6]^{3-}$ in a capped capillary as both an internal standard and lock ($[Al(D_2O)_6]^{3+}$, 0 ppm).[33–37]

^1H NMR spectra were recorded on a JNM-ECA 600 MHz spectrometer with $CDCl_3$ as the solvent. The PIB end-group content was calculated from the ^1H NMR spectra. Fig. 3 shows a typical ^1H NMR spectrum; the main resonance signals are located at $\delta = 1.1$ ppm (z), 1.41 ppm (y), 0.99 ppm (x), 4.85 ppm (a1), 4.64 ppm (a2), 5.17 ppm (c1), 5.37 ppm (c2), 5.15 ppm (d), and 2.83 ppm (e). The two characteristic protons of the exo-olefin end group (structure A, protons a1 and a2) appear as two well-resolved peaks at 4.85 and 4.64 ppm, respectively. Small amounts of the *E* and *Z* configurations of the tri-substituted olefin end group (structure C, protons c1 and c2) appear at 5.37 and 5.17 ppm, respectively. The one characteristic proton of the endo-olefin end group (structure D, proton d) appears at 5.15 ppm. The signal corresponding to the tetra-substituted olefin end group (structure E, proton e) appears as a broad multiplet at 2.85 ppm. The methylene, methyl, and end methyl protons of the PIB chains (structure A, protons y, z, and x, respectively) typically appear at 1.41, 1.11, and 0.99 ppm, respectively.

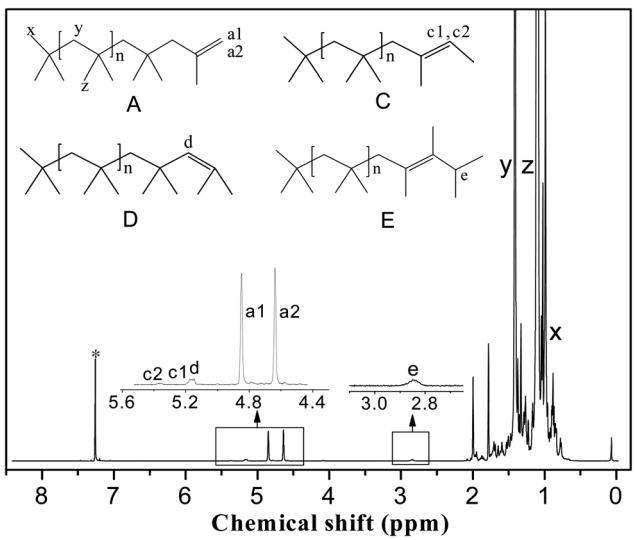

Fig. 3 Typical ^1H NMR spectrum of PIB. The asterisk denotes the $CHCl_3$ resonance.

DFT calculations. The binding energies of different $AlCl_3$/ether complexes were determined by *ab initio* calculations using Gaussian 09W at the B3LYP level of theory. The Pople basis set 6-311G (++, d, p) was used for all atoms in the solvent, and SMD was used as the solvation model.

Results and discussion

Synergistic effects of Et_2O and iPr_2O on $AlCl_3$-initiated IB polymerization in pure *n*-hexane

We first determined the polymerization characteristics using only Et_2O or iPr_2O. The polymerization results are shown in Table 1; method 1 and method 2 correspond to the introduction of only Et_2O and only iPr_2O, respectively. The ether/$AlCl_3$ molar ratio was controlled over unity as a prerequisite to ensuring a high content of exo-olefin according to previous reports on HRPIB synthesis.[8,29,38] As shown in Table 1, the exo-olefinic end-group content (~24%) and yield (~18%) obtained using method 1 are relatively high. In contrast, with method 2, the IB

Table 1 Polymerization of IB catalyzed by $AlCl_3$ with Et_2O or iPr_2O in pure *n*-hexane[a]

Entry	Method	*t* (s)	$[AlCl_3]_I$ (mM)	Conv. (%)	M_n	$Đ$	[PIB]/mM	Exo (%)	Tri + endo (%)	Tetra (%)
1	1	60	10.51	12	5189	2.76	0.82	ND[b]	ND	ND
2		600	10.51	18	4664	4.15	1.41	24	48	28
3	2	60	2.20	3	3828	2.05	0.25	ND	ND	ND
4		600	2.20	5	4074	2.75	0.46	15	85	0

[a] F_{total} = 16 mL min^{-1}; [IB] = 1.3 M; T = 0 °C; $[H_2O]$ = 0 (control) mM, for method 1: $[Et_2O]$ = 15 mM, for method 2: $[iPr_2O]$ = 15 mM. Conv.: gravimetric conversion. [b] Not determined.

conversion and exo-olefinic end-group content were only 3–5% and 15%, respectively. However, in contrast to the initiation solution prepared in CH_2Cl_2 (ε = 9.08),[29] the initiation solution prepared in pure *n*-hexane (ε = 1.89) afforded PIBs mainly containing endo-, tri-, and tetra-substituted double bonds and having polydispersity indices (PDIs) around 2.0 or higher. Meanwhile, the IB conversions were low (<20%) and seemed to be independent of residence time in the range of 60–600 s. We supposed that the $AlCl_3 \cdot Et_2O$ or $AlCl_3 \cdot iPr_2O$ complex could only generate ionic species with low reactivity or poor stability in pure *n*-hexane, which may be attributed to the weak ionization in the nonpolar solvent.[39–41]

Considering that Et_2O or iPr_2O alone did not work for HRPIB preparation in pure *n*-hexane, we attempted to use double ethers to simultaneously regulate the reactivity and stability of ionic species in initiation solution. iPr_2O was expected to stabilize carbenium ions, while Et_2O was expected to promote proton elimination as the key for end group control.

The results of polymerizations utilizing various preparation strategies for initiation solution are summarized in Table 2. For method 3, the IB conversion was similar to that of method 1 (only Et_2O), while the exo-olefin content was reduced to 13%. The subsequent addition of iPr_2O had little influence on the stability and reactivity of growing species mainly coinitiated by $AlCl_3 \cdot Et_2O$ and weakened the β-H elimination effect of Et_2O to some extent. In contrast, when reversing the addition sequence of the two ethers (method 4), the obtained PIBs had a much higher exo-olefin content (up to 35%). This may be attributed to the effect of Et_2O on the proton elimination of growing species mainly coinitiated by $AlCl_3 \cdot iPr_2O$. In addition, since approximately half of the added $AlCl_3$ remained undissolved in method 4, all existing forms of Et_2O in the upper layer were $AlCl_3 \cdot Et_2O$ complexes, which might also play a role in inducing chain initiation and β-H elimination. To confirm this assumption, we used the initiation solution prepared by method 5, in which undissolved $AlCl_3$ at the bottom was removed followed by the addition of Et_2O. As seen in entry 10, the content of exo-olefin end groups decreased slightly to 29%, and the conversion decreased seriously. This indicates that free Et_2O inhibits the reactivity of the growing species coinitiated by $AlCl_3 \cdot iPr_2O$, and $AlCl_3 \cdot Et_2O$ may be critical to facilitate conversion and end group control. Thus, for the growing species coinitiated by $AlCl_3 \cdot iPr_2O$, we speculated that weak ionization in conjunction with slow chain transfer could be overcome by introducing $AlCl_3 \cdot Et_2O$ only. To this end, we removed the free Et_2O during $AlCl_3 \cdot Et_2O$ preparation *via* vacuum to obtain $AlCl_3 \cdot Et_2O$ crystals. Meanwhile, *n*-hexane was added to the $AlCl_3$ powders before adding Et_2O to regulate the interaction between $AlCl_3$ and Et_2O and facilitate the removal of free Et_2O (methods 6 and 7).

As seen in Table 3, the cationic polymerization of IB with methods 6 and 7 in pure *n*-hexane proceeded smoothly; relatively high monomer conversions (21–89%) were achieved within 10 min, affording HRPIBs with comparable contents of exo-olefin terminal groups in the range of 60–75%. The number-average molecular weight (M_n) increased slightly with polymerization time, and the polydispersity index was less than 2.0 in most cases. These results indicate that isomerization *via* carbenium ion rearrangement could be suppressed to some extent. From entries 15 and 16, it is apparent that adding *n*-hexane/Et_2O mixture is important to achieve higher conversion. The addition of *n*-hexane in method 7 may weaken the interaction between $AlCl_3$ and Et_2O, resulting in higher conversion (~89%). This confirmed that the appropriate activity and

Table 2 Polymerization of IB catalyzed by $AlCl_3$ with dual ethers (Et_2O and iPr_2O) in pure *n*-hexane[a]

Entry	Method	*t* (s)	$[AlCl_3]_I$ (mM)	Conv. (%)	M_n	$Đ$	[PIB] (mM)	Exo (%)	Tri + endo (%)	Tetra (%)
5	3	60	11.09	3	ND	ND	ND[b]	ND	ND	ND
6		600	11.09	17	4183	2.94	1.44	13	87	0
7	4	60	8.92	7	3382	3.27	0.77	32	52	16
8		600	8.92	15	3576	2.20	1.54	35	57	8
9	5	60	3.30	3	4126	2.01	0.25	ND	ND	ND
10		600	3.30	4	ND	ND	ND	29	71	0

[a] F_{total} = 16 mL min^{-1}; [IB] = 1.3 M; T = 0 °C; $[H_2O]$ = 0 (control) mM. $[Et_2O]_0$ = 7.86 mM, $[iPr_2O]_0$ = 7.14 mM. Conv.: gravimetric conversion. [b] Not determined.

Table 3 Polymerization of IB catalyzed by $AlCl_3$ with dual ethers (Et_2O and iPr_2O) and a precise ratio of ether/$AlCl_3$ in pure *n*-hexane[a]

Entry	Method	t (s)	$[AlCl_3]_I$ (mM)	Conv. (%)	M_n	$Đ$	[PIB] (mM)	Exo (%)	Tri + endo (%)	Tetra (%)
11	6	60	12.98	5	1271	1.61	1.39	ND[b]	ND	ND
12		600	12.98	21	1464	2.01	5.15	75	19	6
13	7	60	13.21	36	1629	1.91	8.03	60	30	10
14		600	13.21	89	1647	2.23	19.66	52	29	20
15	7–1	60	13.31	6	4117	1.23	0.554	ND	ND	ND
16		600	13.31	33	4302	1.23	2.755	68	20	12

[a] F_{total} = 16 mL min^{-1}; [IB] = 1.3 M; T = 0 °C; $[H_2O]$ = 0 (control) mM. $[Et_2O]_0$ = 7.86 mM, $[iPr_2O]_0$ = 7.14 mM. $[AlCl_3]_A$ = 1.62 mM, Conv.: gravimetric conversion. [b] Not determined.

stability of active species could be obtained by combining double ethers and precise control of the ether/$AlCl_3$ ratio. As a result, HRPIBs could be obtained in under a wide range of IB concentrations (Table 4). To the best of our knowledge, this is the first example of the effective preparation of HRPIBs with $AlCl_3$ as a coinitiator in pure *n*-hexane.

Proposed mechanism of IB polymerization under dual ethers in pure *n*-hexane

In this section, ATR-FTIR and ^{27}Al NMR spectroscopies were used to gain further insight into the role of the dual ethers (Et_2O and iPr_2O). The ATR-FTIR spectra are presented in Fig. 4. The characteristic peak of the C–O bond in free Et_2O is located at 1126 cm^{-1}, while the characteristic peaks of free iPr_2O are situated at 1113, 1126, and 1171 cm^{-1}. For $AlCl_3 \cdot Et_2O$ solution using method 1, the peak at 1126 cm^{-1} was not detected, and two new and broad peaks appeared at 884 and 1005 cm^{-1}. For $AlCl_3 \cdot iPr_2O$ solution using method 2, free iPr_2O molecules still existed. This may be because iPr_2O is present in excess with respect to $AlCl_3$ due to the poor solubility of $AlCl_3$ in iPr_2O with relatively large steric hindrance.

As shown in Fig. 5, when using dual ethers, the characteristic peaks for ether C–O bond stretching were redshifted, and a peak emerged at 999 cm^{-1} (methods 3, 4, 6, and 7), suggesting that the interaction between $AlCl_3$ and C–O was enhanced. More interestingly, the intensities of the peaks around 999 cm^{-1}, which correspond to the Al–O bond, were significantly enhanced in the initiation solutions prepared with methods 6 and 7. This enhancement was positively correlated with the IB conversion. These results suggest that the coinitiators formed in methods 6 and 7 were beneficial for ionizing H_2O and stabilizing the carbocations. However, compared to the different polymerization results obtained using methods 3, 4, 6, and 7, their ATR-FTIR spectra were difficult to distinguish; thus, it is necessary to consider other methods to characterize the interaction between $AlCl_3$ and ether.

To clarify the nature of different $AlCl_3 \cdot$ether complexes, *ab initio* calculations were conducted to determine the $AlCl_3 \cdot$ether binding energies. As shown in Fig. 6, the binding energies between $AlCl_3$ and iPr_2O were 33.07 kcal mol^{-1} in CH_2Cl_2 and 30.49 kcal mol^{-1} in *n*-hexane; the binding energies between $AlCl_3$ and Et_2O were 30.95 kcal mol^{-1} in CH_2Cl_2 and 28.14 kcal mol^{-1} in *n*-hexane. On the other hand, for the same complexes, the binding energies in nonpolar solvent (*n*-hexane) were relatively low. These results indicate that the stability of $AlCl_3 \cdot Et_2O$ was less than that of $AlCl_3 \cdot iPr_2O$, and the stability further decreased with decreasing solvent polarity.

Herein, we further studied the interaction between $AlCl_3$ and ether in *n*-hexane by ^{27}Al NMR spectroscopy (Fig. 7). A single resonance was detected in all cases, indicating that the complexes of $AlCl_3$ and ether or the microenvironment around $AlCl_3$ were uniform. In addition, according to the position of this characteristic peak, the stabilities of the different $AlCl_3$-·ether complexes decreased in the order of method 2, method 4, method 3, method 6, method 7, method 5, and method 1, consistent with the DFT simulations. Methods 6 and 7, which permitted faster polymerization and effective β-H abstraction, resulted in intermediate complex stability.

In detail, the ^{27}Al NMR signal of $AlCl_3 \cdot iPr_2O$ (method 2) shifted even further toward lower frequency (higher field) compared to that of $AlCl_3 \cdot Et_2O$ (method 1). This means that

Table 4 Polymerization of IB catalyzed by $AlCl_3$ with different IB concentrations in *n*-hexane[a]

Entry	[IB] (M)	t (s)	$[AlCl_3]_I$ (mM)	$[AlCl_3]_A$ (mM)	Conv. (%)	M_n	$Đ$	Exo (%)	Tri (%)	Tetra (%)
17	0.33	60	10.98	3.80	29	1880	2.01	73	13	14
18	0.33	600	10.98	3.80	65	1460	2.08	72	15	13
19	0.65	60	11.28	3.75	23	4440	1.91	63	22	15
20	0.65	600	11.28	3.75	56	3730	2.06	58	26	16
21	1.30	60	11.06	3.79	15	6020	2.20	63	20	17
22	1.30	600	11.06	3.79	30	6500	2.25	61	21	18

[a] F_{total} = 16 mL min^{-1}; T = 0 °C; $[H_2O]_0$ = 0.45 mM; $[iPr_2O]_0$ = 7.14 mM. Conv.: gravimetric conversion.

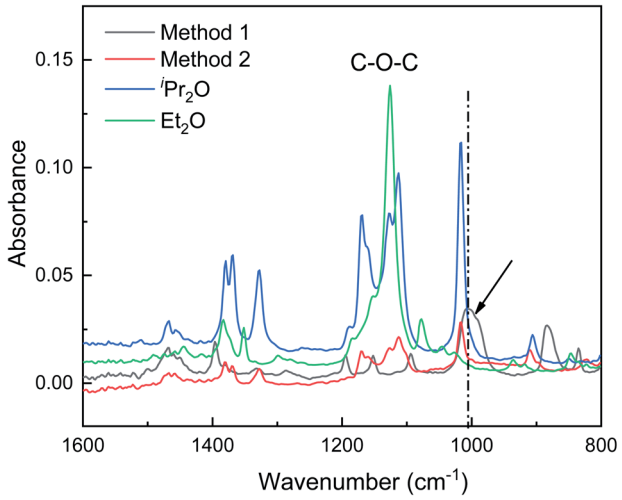

Fig. 4 ATR-FTIR spectra showing the interactions between $AlCl_3$ and ether in initiation solutions prepared with methods 1 and 2. The arrow and dash line indicate the peak corresponding to Al–O bond.

iPr_2O has a stronger electron-donating ability and a greater effect on the microenvironment around the Al atom. In other words, the interaction between $AlCl_3$ and iPr_2O is relatively strong in *n*-hexane, resulting in low reactivity for the ionization of H_2O and inducing transfer side reactions (isomerizations). The interaction between $AlCl_3$ and Et_2O is comparatively weak; thus, the $AlCl_3 \cdot Et_2O$ in $H_2O/AlCl_3 \cdot Et_2O$ initiation system (method 1) has high reactivity for H_2O ionization. However, free Et_2O may promote isomerization and increase the amount of endo-double bond terminal groups in the products. For method 3, weaker $AlCl_3 \cdot Et_2O$ was formed at the first stage, and the subsequently added iPr_2O may distribute around $AlCl_3 \cdot Et_2O$; however, its effect on Al atom may be weak due to steric hindrance. Thus, the microenvironment of the Al atoms was dominated by Et_2O. In contrast, in method 4, stronger

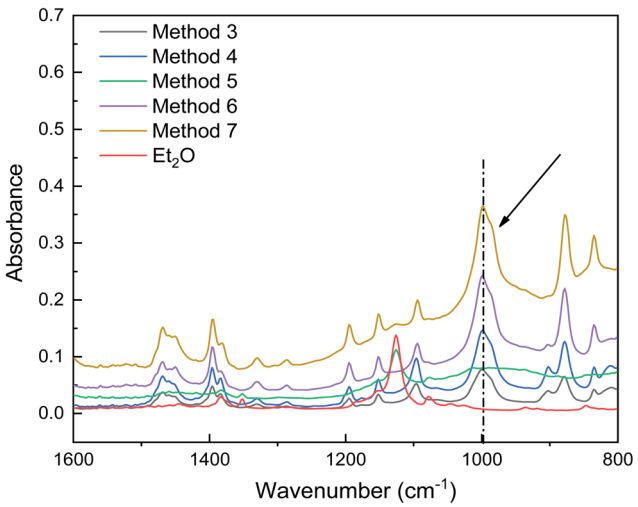

Fig. 5 ATR-FTIR spectra showing the interaction between $AlCl_3$ and ether in initiation solutions prepared using methods 3–7.

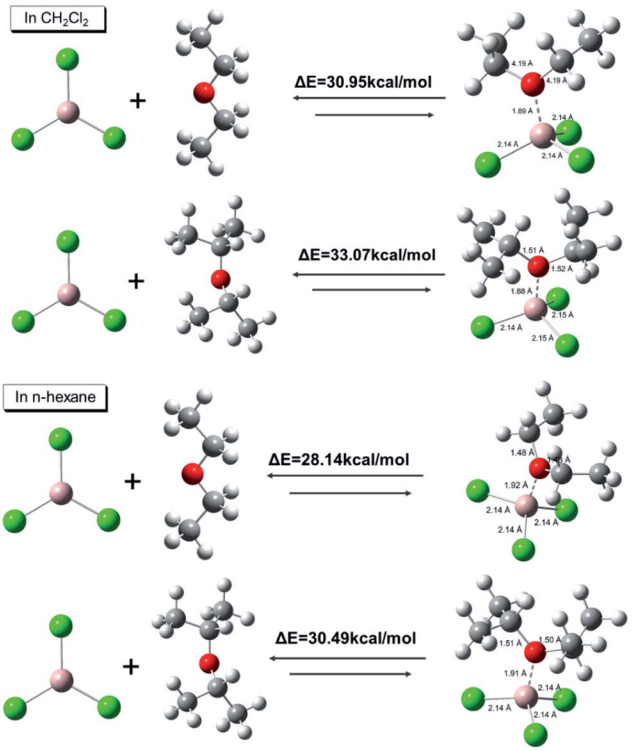

Fig. 6 DFT binding energies and optimized structures of $AlCl_3 \cdot$ether calculated using Gaussian 09W [B3LYP/6-311G (++, d, p), solvation model: SMD]. Distances are in Å.

$AlCl_3 \cdot iPr_2O$ was formed first, and some added Et_2O bound with $AlCl_3$ powder; thus, the microenvironment of Al atom in solution reflected the effect of iPr_2O to some extent. For method 5, all the added free Et_2O was distributed around $AlCl_3 \cdot iPr_2O$, and the interaction between them caused the ^{27}Al shift to be closer to that of $AlCl_3 \cdot Et_2O$. Under the precise control of the $AlCl_3$-$: Et_2O$ ratio (methods 6 and 7), higher activity for $AlCl_3 \cdot iPr_2O$ was endowed by introducing suitable $AlCl_3 \cdot Et_2O$ complex to regulate the micro surroundings of $AlCl_3 \cdot iPr_2O$ properly. In general, the interaction between $AlCl_3$ and Et_2O inhibited the isomerization effect of free Et_2O and regulated the effect of Et_2O on $AlCl_3 \cdot iPr_2O$ toward compromised stability and reactivity.

Based on the above observations, we proposed that $AlCl_3$-$\cdot Et_2O$ might play two roles: participate in the initiation step, which is attributed to the weak interactions between $AlCl_3$ and Et_2O; and accelerate effective β-H elimination since Et_2O was modified by $AlCl_3$. The complexation between $AlCl_3$ and Et_2O may also inhibit the effect of Et_2O on internal proton transfer and abstraction. Meanwhile, $AlCl_3 \cdot iPr_2O$ at a relatively low concentration rarely produced active centers. However, it could modify the stability of cation centers *via* solvation.

Scheme 1 shows the proposed mechanism of the cationic polymerization of IB using the $AlCl_3/Et_2O/iPr_2O$ system in pure *n*-hexane. In detail, modified Et_2O with the assistance of iPr_2O provided the proper microenvironment around $AlCl_3$. $AlCl_3$ then catalyzed the ionization of H_2O and generated considerable stable ionic species. Subsequently, the chain reactions were controlled by the selective β-H abstraction of modified

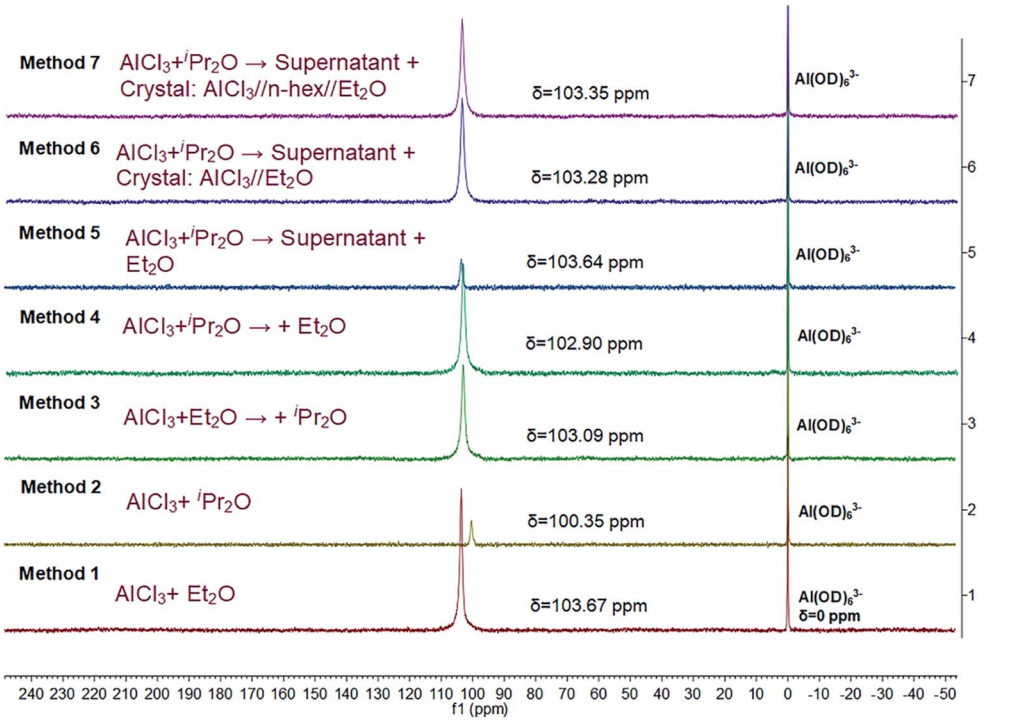

Fig. 7 ^{27}Al NMR spectra of initiation solutions prepared using different methods.

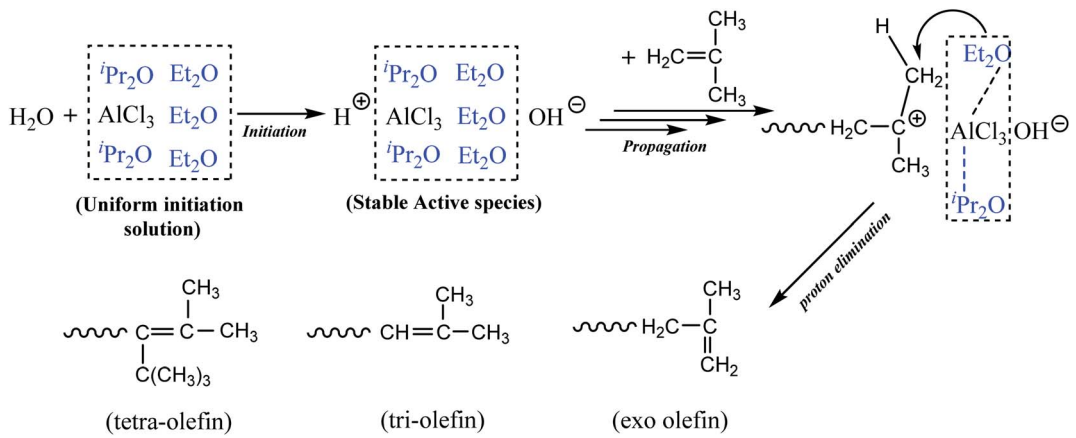

Scheme 1 Proposed mechanism of the cationic polymerization of IB using dual ethers.

Et_2O, resulting in higher conversion and a greater content of exo-olefin. In addition, the use of *n*-hexane weakened the interaction between $AlCl_3$ and Et_2O, facilitating the removal of free Et_2O and inhibiting undesired proton transfer.

Conclusion

In summary, an efficient strategy combining the precise control of the ether/$AlCl_3$ ratio and the use of two nucleophilic reagents (iPr_2O and Et_2O) was developed to synthesize HRPIBs in pure *n*-hexane, resulting in 89% conversion with 60–75% exo-double bond content within 10 min. Among the $AlCl_3$·ether complexes prepared with different preparation methods, good performance in terms of both IB conversion and exo-olefin content was achieved by preparing $AlCl_3 \cdot iPr_2O$ solution and $AlCl_3 \cdot Et_2O$ crystals separately. The various functions of iPr_2O and Et_2O in the initiator solution were comprehensively revealed based on the polymerization results, ATR-FTIR and ^{27}Al NMR spectra, and DFT simulations. The results confirmed that: (1) $AlCl_3 \cdot iPr_2O$ complexes were the key component that stabilized carbenium ions; (2) $AlCl_3 \cdot Et_2O$ complexes were the key component that promoted proton elimination; and (3) free Et_2O had a negative effect on isomerization and should be removed to the extent possible. This new strategy may provide an alternative to commercial BF_3-based initiating systems and lead to commercial interest in HRPIB synthesis in pure green

solvent. In addition, the new method can potentially be extended to other initiation systems containing solid Lewis acids.

Conflicts of interest

There are no conflicts to declare.

Acknowledgements

The authors are thankful for the support of the National Natural Science Foundation of China (Grant No. 21176136, 21422603, and 21978152).

Notes and references

1 K. Kunal, M. Paluch, C. M. Roland, J. E. Puskas, Y. Chen and A. P. Sokolov, *J. Polym. Sci., Part B: Polym. Phys.*, 2008, **46**, 1390–1399.
2 G. K. J. E. Puskas, in *Encyclopedia of Polymer Science and Technology*, Wiley-InterScience, New York, 2003, vol. 5, pp. 382–418.
3 J. P. Kennedy and B. Ivan, *Theory and Practice*, Hanser, Munich, Germany, 1991, pp. 173–177.
4 B. Giese, *Bunsen-Ges. Phys. Chem., Ber.*, 1983, **87**, 289.
5 S. Rach and F. Kühn, *Sustainability*, 2009, **1**, 35–42.
6 I. V. Vasilenko, D. I. Shiman and S. V. Kostjuk, *Polym. Chem.*, 2014, **5**, 3855–3866.
7 R. Kumar, P. Dimitrov, K. J. Bartelson, J. Emert and R. Faust, *Macromolecules*, 2012, **45**, 8598–8603.
8 Q. Liu, Y. Wu, P. Yan, Y. Zhang and R. Xu, *Macromolecules*, 2011, **44**, 1866–1875.
9 P. Dimitrov, J. Emert and R. Faust, *Macromolecules*, 2012, **45**, 3318–3325.
10 H. Mach and P. Rath, *Lubr. Sci.*, 1999, **11**, 175–185.
11 J. J. Harrison, C. M. Mijares, M. T. Cheng and J. Hudson, *Macromolecules*, 2002, **35**, 2494–2500.
12 A. G. Evans and G. W. Meadows, *J. Polym. Sci.*, 1949, **4**, 359–376.
13 L.-b. Zhang, Y.-x. Wu, P. Zhou, G.-y. Wu, W.-t. Yang and D.-s. Yu, *Chin. J. Polym. Sci.*, 2011, **29**, 360–367.
14 S. V. Kostjuk, *RSC Adv.*, 2015, **5**, 13125–13144.
15 A.-R. Guo, X.-J. Yang, P.-F. Yan and Y.-X. Wu, *J. Polym. Sci., Part A: Polym. Chem.*, 2013, **51**, 4200–4212.
16 K. J. Bartelson, P. De, R. Kumar, J. Emert and R. Faust, *Polymer*, 2013, **54**, 4858–4863.
17 R. Kumar, J. Emert and R. Faust, *Polym. Bull.*, 2014, **72**, 49–60.
18 R. Kumar, P. De, B. Zheng, K.-W. Huang, J. Emert and R. Faust, *Polym. Chem.*, 2015, **6**, 322–329.
19 Y. Li, Y. Wu, X. Xu, L. Liang and G. Wu, *J. Polym. Sci., Part A: Polym. Chem.*, 2007, **45**, 3053–3061.
20 Y. Li, Y.-x. Wu, L.-h. Liang, Y. Li and G.-y. Wu, *Chin. J. Polym. Sci.*, 2009, **28**, 55–62.
21 Q. Liu, Y.-X. Wu, Y. Zhang, P.-F. Yan and R.-W. Xu, *Polymer*, 2010, **51**, 5960–5969.
22 I. V. Vasilenko, A. N. Frolov and S. V. Kostjuk, *Macromolecules*, 2010, **43**, 5503–5507.
23 I. V. Vasilenko, D. I. Shiman and S. V. Kostjuk, *J. Polym. Sci., Part A: Polym. Chem.*, 2012, **50**, 750–758.
24 L. B. Zhang, Y. X. Wu, P. Zhou and R. W. Xu, *Polym. Adv. Technol.*, 2012, **23**, 522–528.
25 D. I. Shiman, I. V. Vasilenko and S. V. Kostjuk, *Polymer*, 2013, **54**, 2235–2242.
26 S. V. Kostjuk, I. V. Vasilenko, D. I. Shiman, A. N. Frolov and L. V. Gaponik, *Macromol. Symp.*, 2015, **349**, 94–103.
27 M. Vierle, Y. Zhang, E. Herdtweck, M. Bohnenpoll, O. Nuyken and F. E. Kuhn, *Angew. Chem., Int. Ed. Engl.*, 2003, **42**, 1307–1310.
28 D. I. Shiman, I. V. Vasilenko and S. V. Kostjuk, *J. Polym. Sci., Part A: Polym. Chem.*, 2014, **52**, 2386–2393.
29 S. Zhu, Y. C. Lu, K. Wang and G. S. Luo, *RSC Adv.*, 2016, **6**, 9827–9834.
30 S. Zhu, K. Wang and Y. Lu, *ACS Omega*, 2018, **3**, 2033–2039.
31 S. Zhu, Y. Lu, K. Wang and G. Luo, *RSC Adv.*, 2016, **6**, 97983–97989.
32 D. I. Shiman, I. V. Vasilenko and S. V. Kostjuk, *Polymer*, 2016, **99**, 633–641.
33 J. W. Akitt, *Prog. Nucl. Magn. Reson. Spectrosc.*, 1989, **21**, 1–149.
34 Y. A. Buslaev and S. P. Petrosyants, *Polyhedron*, 1984, **3**, 265–270.
35 D. E. O'Reilly, *J. Chem. Phys.*, 1960, **32**, 1007–1012.
36 H. Haraguch and S. Fujiwara, *J. Phys. Chem.*, 1969, **73**, 3467–3473.
37 D. Chen, K. P. Taylor, Q. Hall and J. M. Kaplan, *Genetics*, 2016, **204**, 1151–1159.
38 Y. Wu and G. Wu, *J. Polym. Sci., Part A: Polym. Chem.*, 2002, **40**, 2209–2214.
39 M. Givehchi, M. Tardi, A. Polton and P. Sigwalt, *Macromolecules*, 2000, **33**, 710–716.
40 K. Matyjaszewski, *Macromol. Symp.*, 1996, **107**, 53–63.
41 I. Dimitrov and R. Faust, *Macromolecules*, 2004, **37**, 9753–9760.

